Transdermal drug delivery by in-skin electroporation using a microneedle array

Keshu Yan, Hiroaki Todo and Kenji Sugibayashi*

Faculty of Pharmaceutical Sciences, Josai University, 1-1 Keyakidai, Sakado, Saitama 350-0295, Japan

* Corresponding author:

Tel.: +81-49-271-7943

Fax: +81-49-271-8137

E-mail: sugib@josai.ac.jp

Abstract

The aim of the present work was to develop a minimally invasive system for the delivery of macromolecular drugs to the deep skin tissues, so called in-skin electroporation (IN-SKIN EP), using a microneedle (MN) electrode array. Fluorescein isothiocyanate (FITC)-dextran (FD-4: average molecular weight, 4.3 kDa) was used as the model macromolecular drug. MNs were arranged to puncture the skin barrier, the stratum corneum, and electrodes were used for EP so that a high electric field could be applied to skin tissues to promote viable skin delivery. *In vitro* skin permeation experiments showed that IN-SKIN EP had a much higher skin penetration-enhancing effect for FD-4 than MN alone or ON-SKIN EP (conventional EP treatment), and that higher permeation was achieved by applying a higher voltage and longer pulse width of EP. In addition, no marked skin irritation was observed by IN-SKIN EP, which was determined by the LDH leaching test.

These results suggest that IN-SKIN EP can be more effectively utilized as a potential skin delivery system of macromolecular drugs than MN alone and conventional ON-SKIN EP.

Keywords: Microneedle; Electroporation; Microneedle electrode; Skin permeation; Skin irritation

1. Introduction

The transdermal drug delivery system (TDDS) is a promising drug formulation that can not only be easily applied without the aid of medical staff compared to injectable formulations, but also offers several advantages, including the elimination of hepatic first-pass metabolism and severe adverse effects on the gastrointestinal tract of oral dosage forms (Jonathan Hadgraft, 1996; Asbill and Michniak, 2000); however, the stratum corneum, the primary barrier to the percutaneous absorption of drugs, has a key function against drug entry into the skin and the systemic circulation of TDDS.

In order to overcome the formidable barrier of the stratum corneum, several physical means have been evaluated in addition to chemical enhancers to promote the skin permeation of drugs. Among the physical means, a microneedle (MN) array can be an effective TDDS due to its advantage of providing a high-performance means to deliver therapeutic drugs through the skin barrier without causing marked skin damage (Kaushik et al., 2001; McAllister et al., 2003). MN arrays can be made of polymers, metal, silicone rubber, polysaccharides and so on, and create new pores in the stratum corneum barrier to increase the permeation pathways of several drugs, including macromolecular drugs (Lin et al., 2001; Matriano et al., 2002; Martanto et al., 2004; Al-Qallaf and Das, 2009; Badran et al.,

2009; Ding et al., 2009; Hafeli et al., 2009; Li et al., 2009); however, such new pathways do not always result in marked skin permeation. We then combined the MN array with iontophoresis (MN-IP), which can be used to increase water flow, because electroosmosis takes place through the skin from the anode to the cathode in the iontophoresis system (Wu et al., 2007). Electroosmosis may be used like a pump syringe for conventional injection (injection system consisting of a needle and pump syringe).

Recently, another physical means, electroporation (EP), has been broadly applied to enhance the skin permeation of drugs. EP involves the creation of tiny and transient aqueous pathways in the transcellular lipid region in the stratum corneum barrier. EP application with a high-voltage electric pulse for a short period (millisecond order) results in the enhanced permeation of high molecular compounds (molecular weight of several hundreds to kilodaltons) through the skin (Medi and Singh, 2003; Fang et al., 2006; Tokumoto et al., 2006; Wong et al., 2006; Marra et al., 2008; Gowrishankar et al., 2009; Sammeta et al., 2009; Xu et al., 2009).

For both MN and EP, in spite of their different mechanisms, enhancement of the skin permeability of drugs is a result of the creation of new permeation pathways in the stratum corneum; however, the pathways do not always persist, so that the skin barrier function is recovered immediately after the pathways close up. TEWL

(transepidermal water loss), as an index of permeability (Zhou et al., 2010), increases after the application of MN or EP and then decreases with time, which explains the recovery of skin barrier function. To prolong the duration of new pathway (pore) openings, longer microneedles were investigated (Zhou et al., 2010) and electrolytes, such as calcium salt, were applied during EP application (Tokudome and Sugibayashi, 2004) for MN and EP studies, respectively.

To achieve a longer duration of pore opening for higher drug permeation in the present study, the mutual synergic action of MN and EP was considered to further increase skin permeation and the bioavailability of macromolecules. The new present combination of MN and EP, so-called in-skin electroporation (IN-SKIN EP), was developed to combine the advantages of MN and EP. An electrically active MN array was created as a device for the present IN-SKIN EP method. Each MN could serve as a microelectrode for EP, which forms an electric field inside the skin barrier. After IN-SKIN EP application, the drug is administered to the skin surface to be delivered into deeper skin tissues. This system is different from conventional EP (ON-SKIN EP), where electrodes are applied just to the skin surface. IN-SKIN EP may facilitate the delivery of high molecular and hydrophilic compounds to deep skin tissues. Furthermore, it affects only a small region of skin, not a wide area of skin by the MN electrode array; thus, IN-SKIN EP probably

increases skin permeability but with low skin irritation.

In the present study, MN puncture of the skin was observed by scanning electron microscopy and confocal laser scanning microscopy. Fluorescein isothiocyanate (FITC)-dextran (FD-4: average molecular weight, 4.3 kDa), which has poor skin permeation due to its high molecular weight and high hydrophilicity, was selected because it could be simply analyzed by a fluorescence spectrophotometer and morphologically observed by a confocal laser fluorescence microscope. The effects of IN-SKIN EP were investigated by *in vitro* skin permeation experiments. The intradermal distribution and skin permeation of FD-4 were determined. In addition, a lactate dehydrogenase (LDH) leakage assay was carried out to evaluate skin damage after IN-SKIN EP pretreatment.

2. Materials and methods

2.1. Chemicals and animals

FD-4 was purchased from Sigma Aldrich (St. Louis, MO, USA). Other chemicals and reagents were of analytical grade and used without further purification.

Male hairless rats (WBM/ILA-Ht, 7–9 weeks old) of approximately 180–250 g were supplied either by the Life Science Research Center, Josai University (Sakado, Saitama, Japan) or Ishikawa Experimental Animal Laboratory (Fukaya,

Saitama, Japan). They were kept at room temperature (25 ± 2°C) with a 12 h light–dark cycle (07:00–19:00 h). All animal experiments were approved by the Institutional Animal Care and Use Committee of Josai University (Sakado, Saitama, Japan).

The hairless rats were anesthetized by peritoneal injection of sodium pentobarbital (50 mg/kg) and hair on the abdomen was carefully shaved using an electric clipper. Abdominal full-thickness skin was excised and adhering fat and connective tissues were carefully eliminated with a ring-ended forceps. The excised skin was confirmed to have no damage, and was immediately used for the experiment.

2.2. Application of IN-SKIN EP using an MN electrode-array

The MN electrode-array for IN-SKIN EP, shown in Fig. 1, was prepared by modification of our previous method (Wu et al., 2007). It was assembled using 9 acupuncture needles (Haruhari, 1.5 mm; Taiho Medical Products Co., Ltd., Hiroshima, Japan), a silicone sheet (15 × 15 ×0.8 mm; Togawa Rubber Co., Ltd., Tokushima, Japan), polyvinyl chloride tape (thickness: 0.2 mm, safety extra low voltage: ~600 V) and a silver sheet (thickness: 0.1 mm), as shown in Fig. 1a. Positive and negative electrodes were set with 4.0-mm spacing arranged alternately, as shown in Fig. 1b. Each needle was 400 μm long with a 28° angle beveled tip, and the base diameter of

the needle was approximately 200 μm, as shown in Fig. 1c. Figure 1d shows a scanning electron micrograph of one MN tip. In order to compare the effect of IN-SKIN EP with conventional ON-SKIN EP, the needle tips of the MN array were filed and struck with a file and hammer to make them obtuse, as shown in Fig. 1e. This obtuse tip needle array was used to apply EP at various points on the skin surface for ON-SKIN EP, so that a similar electric field could be created as a control experiment to research the IN-SKIN EP.

Fig. 1.

The excised skin was manually punctured using the MN electrode-array with vertical pressure of 3.53 N/cm^2 for 10 s for IN-SKIN EP, whereas for ON-SKIN EP, the pressure was set at 0.10 N/cm^2 to ensure that the needle tip did not puncture the skin. This operation was performed on a balance to measure and control the pressure accurately. A pulse generator (ECM 830 Electro Cell Manipulator; BTX, San Diego, CA, USA) was used to provide the square wave of EP (1 pulse/s), at 50–200 V voltage and a pulse width of 10–100 ms.

2.3. In vitro skin permeation experiments

The FD-4 skin permeation experiment was performed after pretreatment of excised hairless rat skin with IN-SKIN EP, ON-SKIN EP or MN alone. The treated skin was mounted on vertical Franz-type diffusion cells (available diffusion area: 1.77 cm^2; volume of receiver cell: 6.0 mL) immediately after treatment, with the stratum corneum side facing the donor compartment and the dermal side facing the receiver compartment. The test FD-4 solution (1.0 mg/mL, 1.0 mL) was added to the donor compartment, whereas phosphate-buffered saline (PBS, pH7.4, 6.0 mL) filled the receiver compartment. The receiver solution was stirred by a magnetic bar to ensure adequate mixing to maintain the sink condition, and was kept at 32 °C with a water jacket.

The solution was sampled at 0.5, 1.0, 2.0, 3.0, 4.0, 5.0, 6.0, 7.0 and 8.0 h after starting the permeation experiment, and an equal volume of fresh PBS was immediately added to keep the volume constant. Intact full-thickness skin (no pretreatment) was also investigated for comparison.

FD-4 concentration in the samples was determined using a fluorospectrophotometer (RF 5300 PC; Shimadzu, Kyoto, Japan) at an excitation wavelength of 495 nm and fluorescent emission wavelength of 515 nm (Wu et al., 2006). The calculated values for the cumulative amount of FD-4 that permeated the skin ($\mu g/cm^2$) were plotted versus time.

2.4. Scanning electron micrographic observation

Scanning electron microscopy (SEM, S-3000N; Hitachi, Tokyo, Japan) was used to observe the skin surface treated by IN-SKIN EP. A skin specimen was mounted on an aluminum stub using double-sided adhesive tape and covered with gold using an ion sputter (E-1010; Hitachi), with the stratum corneum facing up. The samples were observed at 15 kV accelerating voltage, an approximately 20 mm working distance under a 30 Pa vacuum for skin samples.

2.5. Fluorescence confocal microscopic observation

Fluorescence confocal laser scanning was also performed for the excised hairless rat abdominal skin. After the skin permeation experiment, the skin was taken from the diffusion cell and placed in a glass-bottomed dish (Iwaki; Asahi Glass Corp., Funabashi, Chiba, Japan), with the stratum corneum facing down, and FD-4 distribution in the skin was observed using a fluorescence confocal laser scanning microscope (CSM, Fluoview FV1000; Olympus Corp.). Fluorescence from the sample was excited by a 473 nm Hg laser (Rujirat Santipanichwong, 2009). Images were collected using FluoView software (ver. 1.5; Olympus Corp.).

2.6. Confocal microscopic observation

In order to measure the actual depth of pores made by MN alone or IN-SKIN EP, the interior of the skin was observed using a confocal laser scanning microscope (CLS, Vivascope1500, wavelength: 830 nm; Rochester, NY, USA). This instrument can be used to non-invasively observe the interior of tissues. Tissue morphology up to a depth of 350 μm can be observed optically, with high sensitivity and specificity, correlating with histological sectioning (Altintas et al., 2008; Altintas et al., 2009). The punctured areas of excised abdominal skin of hairless rats were observed immediately after puncture with MN alone or IN-SKIN EP.

2.7. Measurement of lactate dehydrogenase (LDH) leakage from pretreated skin in vivo

Hairless rats were anesthetized by *s.c.* injection of urethane (1.0 mg/kg), and hair on the abdomen was carefully removed using an electric clipper. A glass cell cap was attached using adhesive (Aronalpha; Toagosei, Tokyo, Japan) after pretreatment with IN-SKIN EP. Earle's balanced salt solution (EBSS, 2.0 mL) was then added to the glass cell cap. Whole solution was periodically collected from the glass cap cell, and the same volume of blank EBSS was added to keep the volume constant. LDH leached from the stratum corneum side was determined by an assay

kit (Lactate Dehydrogenase Cytotoxicity Assay Kit; Cayman, MI, USA). Non-pretreated intact skin and stripped skin were also investigated for comparison. The stripped skin was made by stripping the stratum corneum 20 times with tape. All experiments were carried out *in vivo*.

2. 8. Statistical analysis

Statistical analysis was performed using the unpaired Student's t-test. Significant difference was accepted at 0.05. ANOVA was also applied in this study (Tokumoto et al., 2005).

3. Results and discussion

3.1. Effect of IN-SKIN EP pretreatment on the skin permeation of FD-4

Figure 2 shows the time course of the cumulative amount of FD-4 that permeated skin pretreated with MN, ON-SKIN EP (200 V, 10 ms, 10 pulses) or IN-SKIN EP (200 V, 10 ms, 10 pulses). The control experiment (no pretreatment) is also shown and was performed to establish a technique with reproducible results. Significant differences were found in the permeation profiles between control and pretreatment groups. Little FD-4 (0.03 μg/cm^2) permeated intact skin over 8 h, whereas MN and ON-SKIN EP pretreatment enhanced the permeability

approximately 7-fold (0.20 μg/cm^2) and 20-fold (0.61 μg/cm^2), respectively. Furthermore, IN-SKIN EP showed 140-fold (4.17 μg/cm^2) permeability compared with the control permeation, suggesting a great synergistic effect of MN and EP on the skin permeation of FD-4. These results, together with correlative results by conventional EP (Catherine Lombry et al., 2000; Tokudome and Sugibayashi, 2003) indicate that IN-SKIN EP resulted in higher drug permeability with a lower voltage or shorter pulse width of EP. In addition, a higher skin penetration-enhancing effect could be obtained with IN-SKIN EP than with the previous MN-IP treatment (Wu et al., 2007), even though the permeation experiment for *in vitro* MN-IP treatment continued for 15 h.

Fig. 2.

Figure 3 shows scanning electron micrographs of intact skin (a) and skin pretreated with MN (b), ON-SKIN EP (200 V, 10 ms, 10 pulses) (c) and IN-SKIN EP (200 V, 10 ms, 10 pulses) (d). The surface of skin pretreated with IN-SKIN EP was observed to assess the effect of IN-SKIN EP to produce a transport channel across the primary barrier, the stratum corneum, against drug entry to viable tissues. The diameter of the newly produced transport channels was measured horizontally and

vertically, and their average size was used as an index of channel size. The average diameter of the channel produced by MN alone was 77.65 μm (Fig. 3b), and that by ON-SKIN EP was 168.83 μm (Fig. 3c), but no distinct channel was produced by ON-SKIN EP. The average diameter of the channel with IN-SKIN EP pretreatment was 166.20 μm (Fig. 3d). IN-SKIN EP produced the largest and deepest pore channels in skin, among the methods in the present study, and these channels would be new effective permeation pathways for chemical compounds, even macromolecules.

Fig. 3.

Intradermal distribution of FD-4 after IN-SKIN EP pretreatment was also investigated using a confocal fluorescein microscope (CSM). Figure 4 shows fluorescein CSM images of skin sections. It is known from the present *in vitro* skin permeation experiments that the cumulative amount of FD-4 permeated was very limited in intact skin (Fig. 2). Correspondingly, in Fig. 4a, the average depth of fluorescent part is 20-30 μm, so it can be considered that FD-4 is only distributed on the skin and in the stratum corneum but not permeating to the deep part. In the skin pretreated with MN (Fig. 4b), the arrow shows puncture site by MN, where the

fluorescence front was about 60 μm depth. In ON-SKIN EP (EP condition: 200 V, 10 ms, 10 pulses) (Fig. 4c), the fluorescence was distributed averagely deeper than intact skin or MN pretreatment. The thickness of green fluorescence in Fig. 4a-c was well correlated to the skin permeation of FD-4 as shown in Fig. 2. Although only a little difference was found among the picture in Fig. 4a-c, much deeper green trails could be clearly observed through the transport channel in skin pretreated with IN-SKIN EP (EP condition: 200 V, 10 ms, 10 pulses) (Fig. 4d). FD-4 was effectively delivered to the deep part of skin in IN-SKIN EP.

Fig. 4.

The pore channel below the skin surface produced by MN alone and IN-SKIN EP was observed by a confocal microscope. A series of pictures was taken from the surface to the deep part of the skin to analyze the depth of pores made by MN alone or IN-SKIN EP. Figure 5a–c shows skin pores (arrow) of 0.00, 10.96, and 65.85 μm depth, respectively, with MN alone. No pore was found in the depth of 65.85 μm (dotted line arrow). Although the MN electrode was 400 μm long (Fig. 1c), pore depth was less than 1/6 the full length of the MN, probably due to skin elasticity. Hairless rat skin consists of three layers: stratum corneum (approximately

0–10 μm), viable epidermis (approximately 60–90 μm) and dermis (>90 μm) (Bouclier et al., 1987). Thus, MN tips reached the viable epidermis and bypassed the stratum corneum. The holes punctured by MN therefore act as a permeation pathway for high molecular compounds.

The pores made by IN-SKIN EP were also observed. Figure 5d–f shows a similar set of images for IN-SKIN EP pretreatment to Fig. 5a–c for MN alone. EP conditions were 200 V, 10 msec and 10 pulses. Compared to Fig. 5a–c, the pores made by IN-SKIN EP were much larger and deeper. Limited by the quality of the images, data were collected until a depth of 79.84 μm (Fig. 5f). The pore could still be observed in the recorded depth. These data show a coincidence in depth with Fig. 4b and d. In addition, the zone of the puncture periphery, which was a circular region of approximately 100-μm diameter, was dark in the images. This could be considered a type of change in skin tissues, such as localized transport regions (LTR), as well as the Joule heat effect. Although evidence of the creation of these LTRs is still indirect in the present study, this zone is also considered as the effect of EP and acts as an important part of drug permeation (Pliquett et al., 1996; Prausnitz, 1996; Zewert et al., 1999; Denet et al., 2004).

Fig. 5.

3. 2. Effect of voltage and pulse width on IN-SKIN EP treatment

Figure 6 shows the effect of the application voltage and pulse width of EP on the cumulative amounts of FD-4 that permeated skin pretreated by IN-SKIN EP (over 8 h). Voltage, pulse width and the number of pulses are the three most important parameters of the EP effect on skin permeation (Sharma et al., 1999). In this study, the effective application period of IN-SKIN EP was fixed to 10 s, and the square wave pulse was applied at 1 pulse/s, so the number of pulses became 10. When the voltage condition was 0, 50, 100 or 150 V under a pulse width of 10 ms, the cumulative amount of FD-4 skin permeation over 8 h was 0.20 ± 0.05, 0.23 ± 0.03, 0.64 ± 0.19 or 1.35 ± 0.91 μg/cm^2, respectively. When the pulse width was fixed to 50 ms and the voltage condition was 50, 100 or 150 V, the cumulative amount over 8 h was 0.33 ± 0.03, 0.81 ± 0.13 or 1.96 ± 0.64 μg/cm^2, respectively. Based on these data, the cumulative amount over 8 h increased with the increase in applied voltage with convex downward. When the voltage was increased to 200 V, the cumulative amount increased steeply. When the voltage condition was 50 or 100 V at a pulse width of 100 ms, the cumulative amount over 8 h was 0.68 ± 0.18 or 3.00 ± 0.12 μg/cm^2, respectively. Increasing the pulse width to 100 ms is therefore an effective way to achieve a high cumulative permeation drug amount, even at a lower voltage.

Although either the voltage or pulse width could markedly contribute to FD-4 permeability through excised hairless rat skin, 200 V and 10 ms pulse width showed the highest FD-4 permeation among the conditions evaluated in this study. No data are shown for severe IN-SKIN EP conditions, such as high voltage (> 200 V) or long pulse width (> 100 ms), since the sink condition could not be maintained in the receiver solution over 8 h due to the extremely high skin permeation of FD-4.

Although the effect of molecular weight of a drug or compound is always considered an important factor in the research of transdermal drug delivery, FD-4 was used as a model compound to evaluate a new combination of MN and EP. Based on the results in the present study, other model compounds with larger molecular weight will also be investigated in the following study.

Fig. 6.

3.3. Influence of IN-SKIN EP on lactate dehydrogenase (LDH) leaching from skin

EP application was found to increase tissue temperature due to Joule heating (Becker and Kuznetsov, 2007). It was considered from the present SEM images that a certain level of scorching was found in pores punctured by IN-SKIN EP. Cutaneous cells may be damaged when the skin is punctured by IN-SKIN EP. In

order to estimate the irritation caused by IN-SKIN EP, LDH leaching from the skin was determined. The LDH leaching was used to assess skin viability (Messager et al., 2003; Wu et al., 2006) in order to evaluate the safety of different physical enhancing methods. Two strong EP conditions (200 V, 10 ms, 10 pulses and 100 V, 100 ms, 10 pulses) were evaluated. Stripped skin was also evaluated for comparison. Figure 7 shows the cumulative amount of LDH leakage from the skin surface over 1, 4 and 8 h after pretreatment. The cumulative amount of LDH leaching from stripped skin was 6.6 times that of intact skin over 8 h. In contrast, no significant difference was found between intact skin and either of the pretreatment conditions; therefore, in the present study, it can be concluded that IN-SKIN EP could create a novel permeation route to enhance penetration with little damage to skin cells. Histological investigation is necessary to evaluate the safety of the IN-SKIN EP method in detail.

Fig. 7.

4. Conclusions

In order to deliver macromolecules through skin, it is important to surmount the stratum corneum barrier to increase permeability. To address this challenge, a

novel IN-SKIN EP was developed in this research. From the present results of the *in vitro* skin permeation of FD-4, it was concluded that treatment with MN or ON-SKIN EP alone increased the permeation of FD-4 through excised hairless rat skin, and IN-SKIN EP further increased skin permeation, which was considered a great synergistic effect of MN and ON-SKIN EP. In particular, higher permeation was achieved when applying higher voltage and longer pulse width EP. The skin distribution of FD-4 indicated the centrality of the EP application site in this system. In the present study, the low irritation of IN-SKIN EP could be concluded from the LDH experiment.

In conclusion, IN-SKIN EP can effectively deliver high molecular and hydrophilic drugs. Not only drug solutions but also the topical formulations, such as gel, ointment or a patch can be applied after pretreatment with IN-SKIN EP, and could be more convenient for clinical application.

References

Al-Qallaf, B., Das, D. B., 2009. Optimizing microneedle arrays to increase skin permeability for transdermal drug delivery. Ann. N. Y. Acad. Sci. 1161, 83-94.

Altintas, M. A., Altintas, A. A., Guggenheim, M., Knobloch, K., Niederbichler, A. D., Vogt, P. M., 2008. Monitoring of microcirculation in free transferred musculocutaneous latissimus dorsi flaps by confocal laser scanning microscopy - a promising non-invasive methodical approach. J. Plast. Reconstr. Aesthet. Surg. 63, 111-117.

Altintas, M. A., Altintas, A. A., Knobloch, K., Guggenheim, M., Zweifel, C. J., Vogt, P. M., 2009. Differentiation of superficial-partial vs. deep-partial thickness burn injuries in vivo by confocal-laser-scanning microscopy. Burns 35, 80-86.

Asbill, C. S., Michniak, B. B., 2000. Percutaneous penetration enhancers: local versus transdermal activity. Pharm. Sci. Technolo. Today 3, 36-41.

Badran, M. M., Kuntsche, J., Fahr, A., 2009. Skin penetration enhancement by a microneedle device (Dermaroller) in vitro: dependency on needle size and applied formulation. Eur. J. Pharm. Sci. 36, 511-523.

Becker, S. M., Kuznetsov, A. V., 2007. Thermal damage reduction associated with in vivo skin electroporation: A numerical investigation justifying aggressive pre-cooling. Int. J. Heat Mass Transf. 50, 105-116.

Bouclier, M., Jomard, A., Kail, N., Shroot, B., Hensby, C., 1987. Induction of ornithine decarboxylase activity in hairless rat epidermis as a pharmacological model: validation of the animal model. Lab. Anim. 21, 233-240.

Catherine Lombry, Nathalie Dujardin, Pre´at, V. r., 2000. Transdermal Delivery of Macromolecules Using Skin Electroporation. Pharm. Res. 17, 32-37.

Denet, A. R., Vanbever, R., Preat, V., 2004. Skin electroporation for transdermal and topical delivery. Adv. Drug. Deliv. Rev. 56, 659-674.

Ding, Z., Verbaan, F. J., Bivas-Benita, M., Bungener, L., Huckriede, A., van den Berg, D. J., Kersten, G., Bouwstra, J. A., 2009. Microneedle arrays for the transcutaneous immunization of diphtheria and influenza in BALB/c mice. J.

Control. Release 136, 71-78.

Fang, J. Y., Hung, C. F., Hwang, T. L., Wong, W. W., 2006. Transdermal delivery of tea catechins by electrically assisted methods. Skin. Pharmacol. Physiol. 19, 28-37.

Gowrishankar, T. R., Herndon, T. O., Weaver, J. C., 2009. Transdermal drug delivery by localized intervention. IEEE. Eng. Med. Biol. Mag. 28, 55-63.

Hafeli, U. O., Mokhtari, A., Liepmann, D., Stoeber, B., 2009. In vivo evaluation of a microneedle-based miniature syringe for intradermal drug delivery. Biomed. Microdevices 11, 943–950.

Jonathan Hadgraft, J. P., Dafydd G. Williams, W. John Pugh, Geoffrey Allan, 1996. Mechanisms of action of skin penetration enhancers/retarders: Azone and analogues. Int. J. Pharm. 141, 17-25.

Kaushik, S., Hord, A. H., Denson, D. D., McAllister, D. V., Smitra, S., Allen, M. G., Prausnitz, M. R., 2001. Lack of pain associated with microfabricated microneedles. Anesth. Analg. 92, 502-504.

Li, G., Badkar, A., Nema, S., Kolli, C. S., Banga, A. K., 2009. In vitro transdermal delivery of therapeutic antibodies using maltose microneedles. Int. J. Pharm. 368, 109-115.

Lin, W., Cormier, M., Samiee, A., Griffin, A., Johnson, B., Teng, C. L., Hardee, G. E., Daddona, P. E., 2001. Transdermal delivery of antisense oligonucleotides with microprojection patch (Macroflux) technology. Pharm. Res. 18, 1789-1793.

Marra, F., Levy, J. L., Santi, P., Kalia, Y. N., 2008. In vitro evaluation of the effect of electrotreatment on skin permeability. J. Cosmet. Dermatol. 7, 105-111.

Martanto, W., Davis, S. P., Holiday, N. R., Wang, J., Gill, H. S., Prausnitz, M. R., 2004. Transdermal delivery of insulin using microneedles in vivo. Pharm. Res. 21, 947-952.

Matriano, J. A., Cormier, M., Johnson, J., Young, W. A., Buttery, M., Nyam, K., Daddona, P. E., 2002. Macroflux microprojection array patch technology: a

new and efficient approach for intracutaneous immunization. Pharm. Res. 19, 63-70.

McAllister, D. V., Wang, P. M., Davis, S. P., Park, J. H., Canatella, P. J., Allen, M. G., Prausnitz, M. R., 2003. Microfabricated needles for transdermal delivery of macromolecules and nanoparticles: fabrication methods and transport studies. Proc. Natl. Acad. Sci. U. S. A. 100, 13755-13760.

Medi, B. M., Singh, J., 2003. Electronically facilitated transdermal delivery of human parathyroid hormone (1-34). Int. J. Pharm. 263, 25-33.

Messager, S., Hann, A. C., Goddard, P. A., Dettmar, P. W., Maillard, J. Y., 2003. Assessment of skin viability: is it necessary to use different methodologies? Skin Res Technol 9, 321-330.

Pliquett, U. F., Zewert, T. E., Chen, T., Langer, R., Weaver, J. C., 1996. Imaging of fluorescent molecule and small ion transport through human stratum corneum during high voltage pulsing: localized transport regions are involved. Biophys. Chem. 58, 185-204.

Prausnitz, M. R., 1996. The effects of electric current applied to skin: A review for transdermal drug delivery. Adv. Drug. Deliv. Rev. 18, 395-425.

Rujirat Santipanichwong, M. S., 2009. Influence of different β-glucans on the physical and rheological properties of egg yolk stabilized oil-in-water emulsions. Food Hydrocolloids 23, 1279-1287

Sammeta, S. M., Vaka, S. R., Narasimha Murthy, S., 2009. Transdermal drug delivery enhanced by low voltage electropulsation (LVE). Pharm. Dev. Technol. 14, 159-164.

Sharma, A., Kara, M., Smith, F. R., Krishinan, T. R., 1999. Transdermal Drug Delivery Using Electroporation. I. Factors Influencing In Vitro Delivery of Terazosin Hydrochloride in Hairless Rats. J. Pharm. Sci. 89, 528-535.

Tokudome, Y., Sugibayashi, K., 2003. The effects of calcium chloride and sodium chloride on the electroporation-mediated skin permeation of fluorescein isothiocyanate (FITC)-dextrans in vitro. Biol. Pharm. Bull. 26, 1508-1510.

Tokudome, Y., Sugibayashi, K., 2004. Mechanism of the synergic effects of calcium chloride and electroporation on the in vitro enhanced skin permeation of drugs. J. Control. Release 95, 267-274.

Tokumoto, S., Higo, N., Sugibayashi, K., 2006. Effect of electroporation and pH on the iontophoretic transdermal delivery of human insulin. Int. J. Pharm. 326, 13-19.

Tokumoto, S., Mori, K., Higo, N., Sugibayashi, K., 2005. Effect of electroporation on the electroosmosis across hairless mouse skin in vitro. J. Control. Release 105, 296-304.

Wong, T. W., Chen, C. H., Huang, C. C., Lin, C. D., Hui, S. W., 2006. Painless electroporation with a new needle-free microelectrode array to enhance transdermal drug delivery. J. Control. Release 110, 557-565.

Wu, X. M., Todo, H., Sugibayashi, K., 2006. Effects of pretreatment of needle puncture and sandpaper abrasion on the in vitro skin permeation of fluorescein isothiocyanate (FITC)-dextran. Int. J. Pharm. 316, 102-108.

Wu, X. M., Todo, H., Sugibayashi, K., 2007. Enhancement of skin permeation of high molecular compounds by a combination of microneedle pretreatment and iontophoresis. J. Control. Release 118, 189-195.

Xu, Q., Kochambilli, R. P., Song, Y., Hao, J., Higuchi, W. I., Li, S. K., 2009. Effects of alternating current frequency and permeation enhancers upon human epidermal membrane. Int. J. Pharm. 372, 24-32.

Zewert, T. E., Pliquett, U. F., Vanbever, R., Langer, R., Weaver, J. C., 1999. Creation of transdermal pathways for macromolecule transport by skin electroporation and a low toxicity, pathway-enlarging molecule. Bioelectrochem Bioenerg. 49, 11-20.

Zhou, C. P., Liu, Y. L., Wang, H. L., Zhang, P. X., Zhang, J. L., 2010. Transdermal delivery of insulin using microneedle rollers in vivo. Int. J. Pharm. 392, 127-133.

Figure legends

Fig. 1. Schematic illustration of MN electrode-array made by acupuncture needles. a) Top view, b) Back view, c) Side view, d) Microphotograph of needle tip, e) Microphotograph of obtuse needle tip for ON-SKIN EP.

Fig. 2. Time course of the cumulative amount of FD-4 that permeated intact skin, skin treated with MN alone, skin treated with ON-SKIN EP and skin treated with IN-SKIN EP. Symbols: ◇, no pretreatment (intact skin); □, MN alone; △, ON-SKIN EP (200 V, 10 ms, 10 pulses); ●, IN-SKIN EP (200 V, 10 ms, 10 pulses). Each data point represents the mean ± S.E. of four or five experiments.

Fig. 3. SEM microphotograph of pores on the skin surface after pretreatment. a) Intact skin, b) MN alone, c) ON-SKIN EP (200 V, 10 ms, 10 pulses), d) IN-SKIN EP (200 V, 10 ms, 10 pulses).

Fig. 4. Fluorescence confocal laser scanning microscopy (CSM) images of FD-4 distribution after 8 h permeating intact and pretreated skin. a) Intact skin, b) MN only, c) ON-SKIN EP (200 V, 10 ms, 10 pulses), d) IN-SKIN EP (200 V, 10 ms, 10 pulses).

Fig. 5. Confocal laser scanning microscopy (CLS) images in the puncture direction of the pore punctured by MN alone (a–c) and IN-SKIN EP (d-f). Depth: a) 0.00 μm, b) 10.96 μm, c) 65.85 μm, d) 0.00 μm, e) 49.90 μm, f) 79.84 μm.

Fig. 6. Effect of pulse width and voltage of EP on the time course of the cumulative amount of FD-4 that permeated hairless rat skin. Symbols: ◆, 10 ms; ■, 50 ms; ▲, 100ms. Each data point represents the mean ± S.E. of four or five experiments.

Fig. 7. Effect of different pretreatments on LDH leaching from the skin surface. Each point represents the mean ± S.E. of three or four experiments. (*: < 0.05; **: < 0.01) □ Intact skin, ▒ MN-EP (200 V, 10 ms), ▒ MN-EP (100 V, 100 ms) and ■ Stripped skin.

Fig. 1

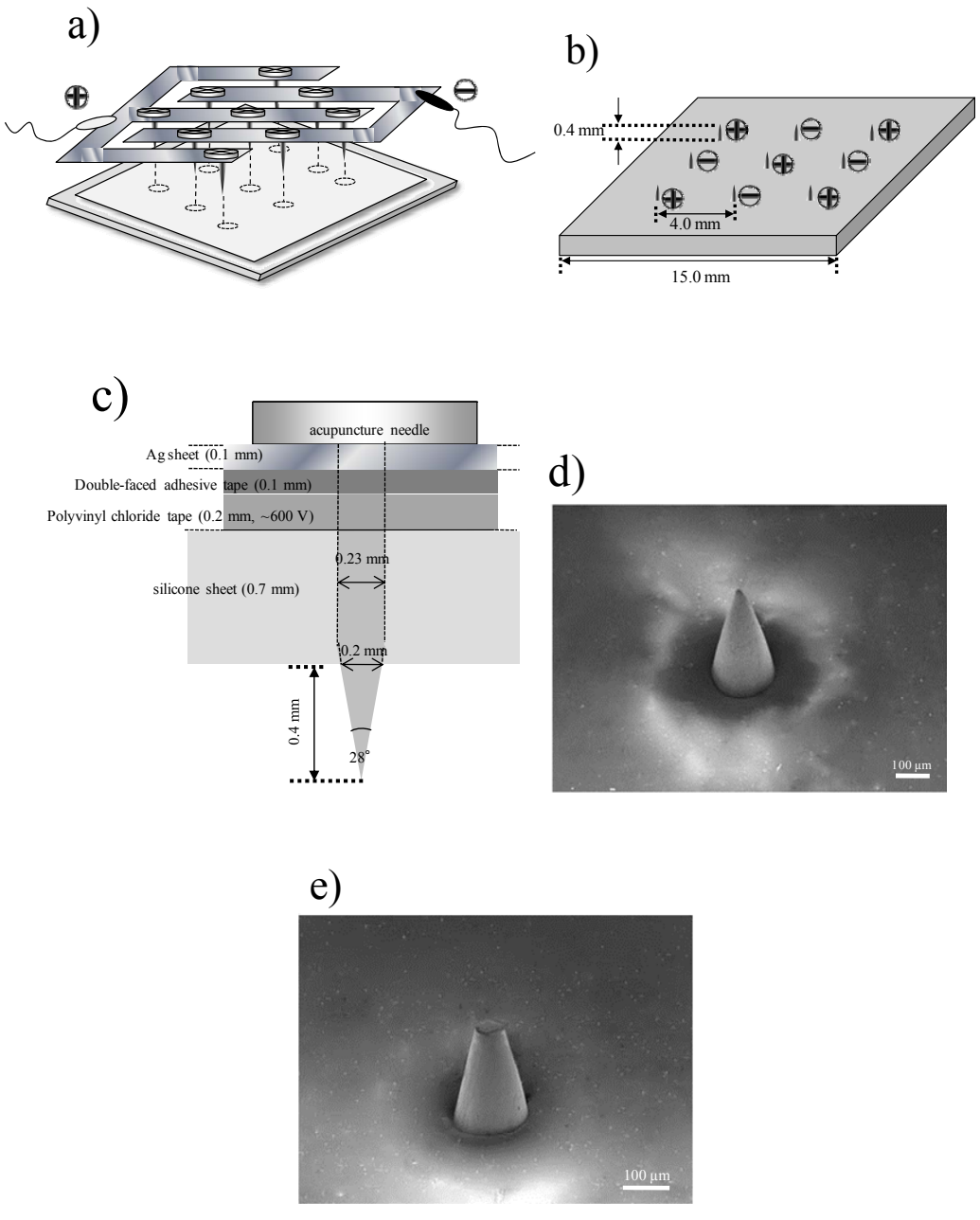
a)
b)
0.4 mm
4.0 mm
15.0 mm
c)
acupuncture needle
Ag sheet (0.1 mm)
Double-faced adhesive tape (0.1 mm)
Polyvinyl chloride tape (0.2 mm, ~600 V)
0.23 mm
silicone sheet (0.7 mm)
0.2 mm
0.4 mm
28°
d)
100 μm
e)
100 μm

Fig. 2

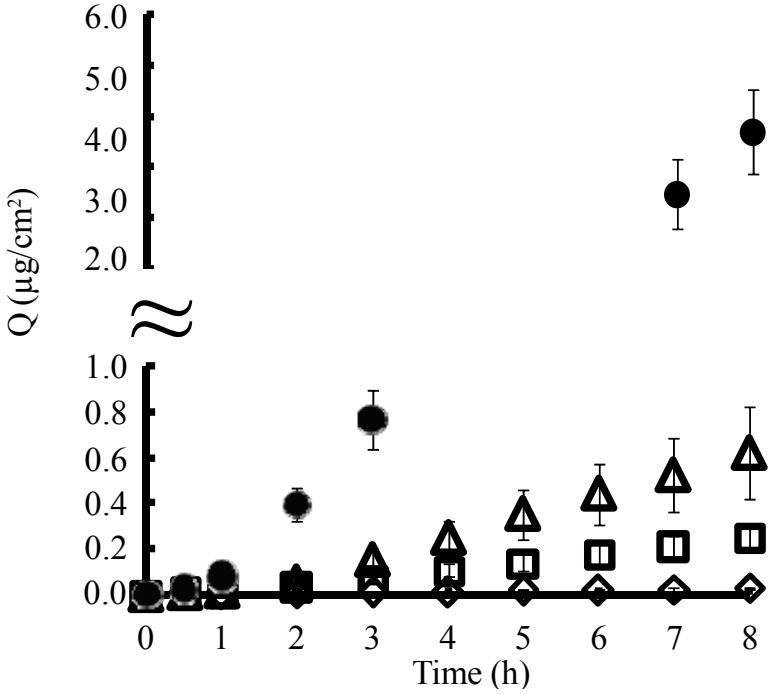

Fig. 3

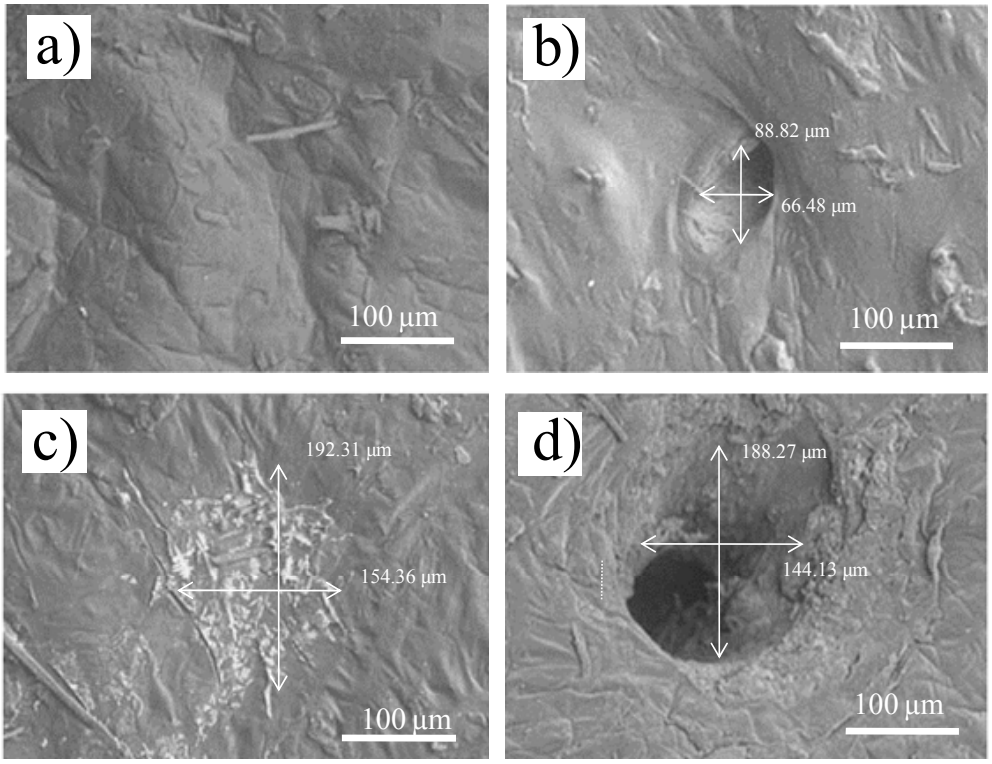
a)
100 µm
b)
88.82 µm
66.48 µm
100 µm
c)
192.31 µm
154.36 µm
100 µm
d)
188.27 µm
144.13 µm
100 µm

Fig. 4

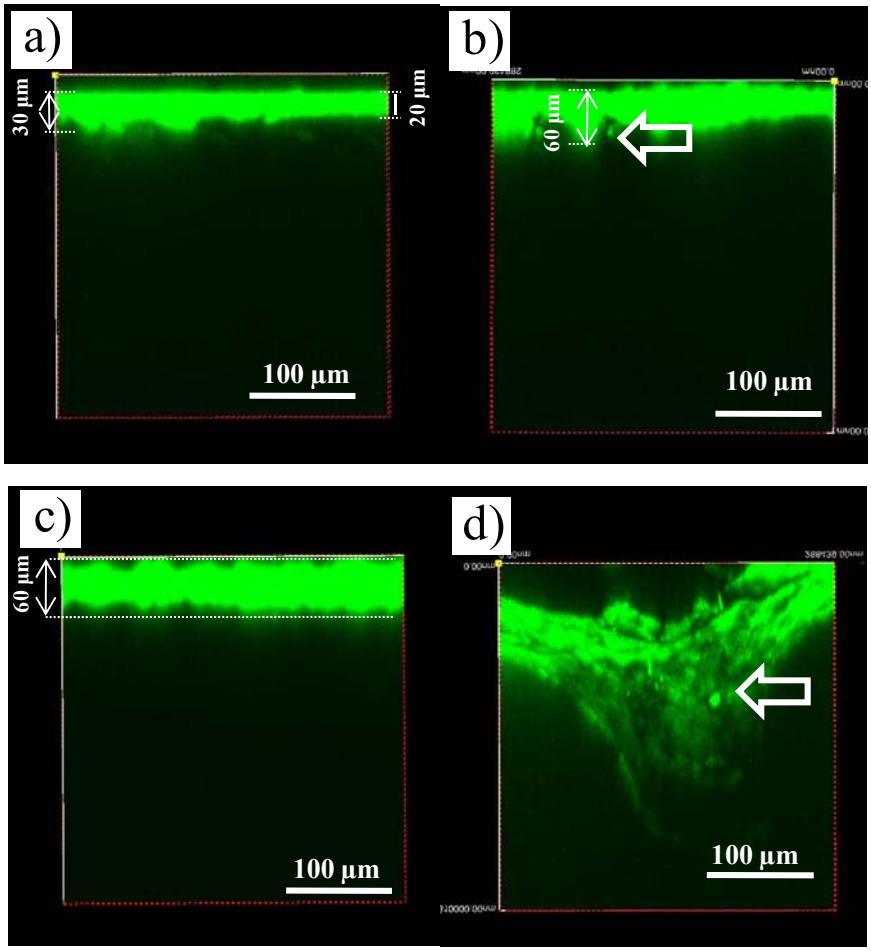

Fig. 5

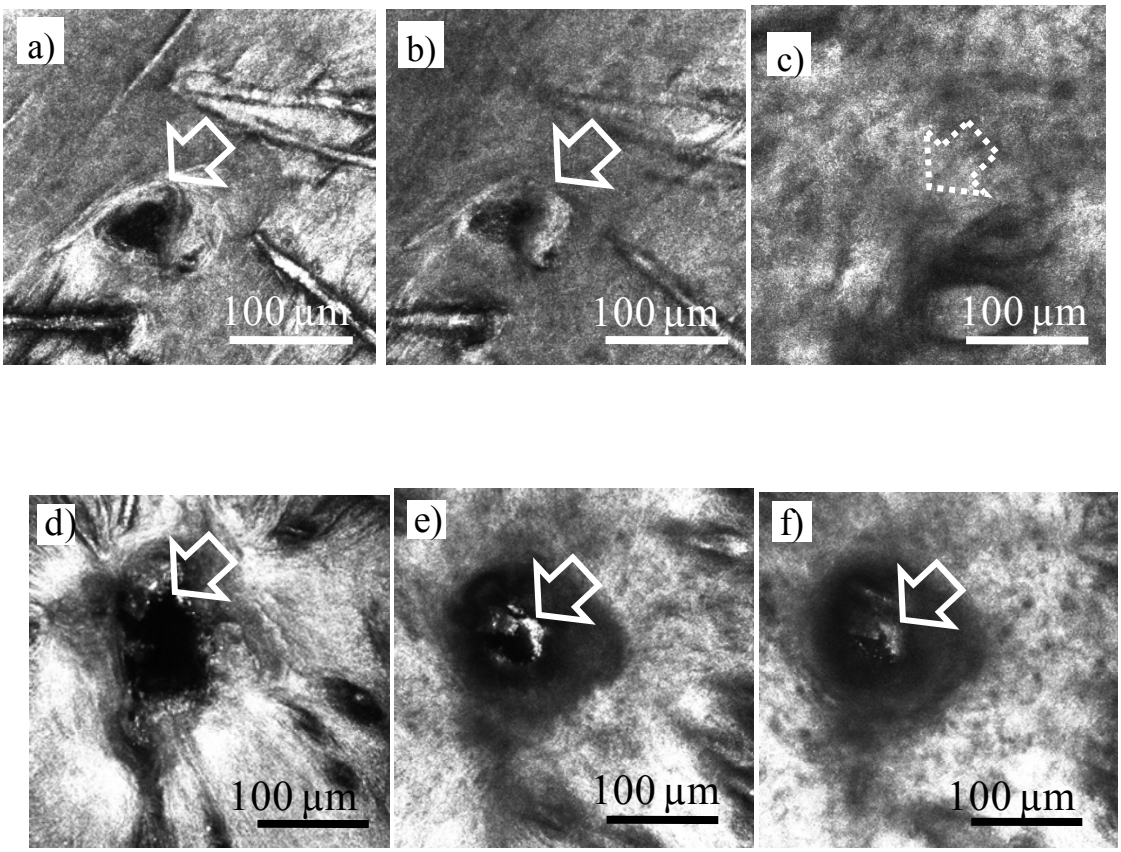

Fig. 6

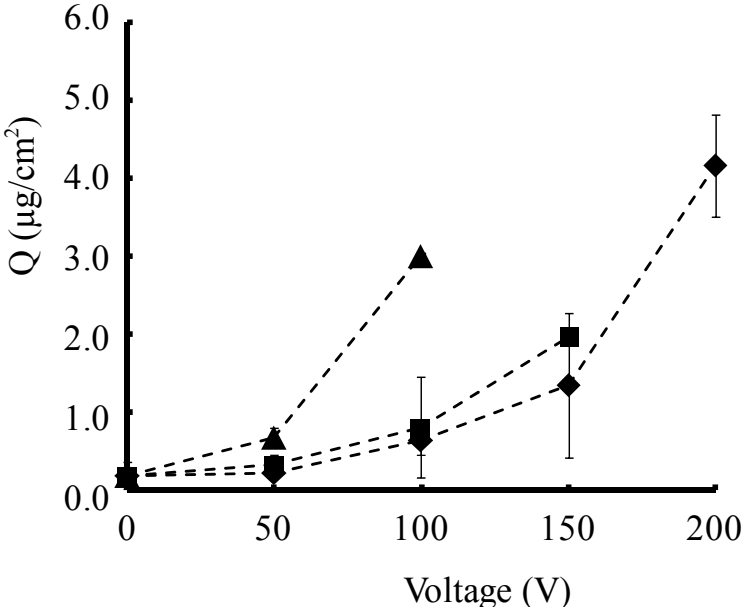

Fig. 7